Energy 356 (2026) 141177

Contents lists available at ScienceDirect

Energy

journal homepage: www.elsevier.com/locate/energy

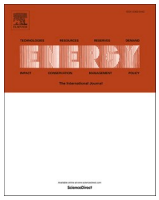

Flexibility through thermal energy storage: cost-effective electrification of European district heating networks

Alexander Burkhardt [a,b,*], Miriam Frömel [a,b], Gerda Deac [a], Anna Billerbeck [a]

[a] Fraunhofer Institute for Systems and Innovation Research ISI, Breslauer Strasse 48, 76139, Karlsruhe, Germany
[b] Karlsruhe Institute of Technology (KIT), Institute for Industrial Production (IIP), Hertzstrasse 16, 76187, Karlsruhe, Germany

ARTICLE INFO

Keywords:
energy system modelling
Optimisation
District heating
thermal energy storage
Flexibility

ABSTRACT

Climate-neutral energy systems require flexibility to integrate variable renewable energy while meeting seasonal heat demand. We integrate tank thermal energy storage (TTES) and pit thermal energy storage (PTES) with dynamic self-discharge modelling in the European energy system model Enertile to address gaps in existing studies that rely on static efficiency assumptions. We analyse three main scenarios for 2050: (1) a baseline without thermal energy storage (TES), (2) a scenario with TTES, and (3) a scenario with PTES deployment. Our results show that TES enables deeper district heating electrification: Heat pump generation increases by 46%, hydrogen boilers are replaced, and biomass capacity is reduced by 51%. Contrary to static-efficiency studies that predict seasonal operation, PTES operates in monthly cycles and TTES in biweekly cycles. TES shifts Power-to-Heat electricity consumption to low electricity-cost periods, reduces curtailment, and decreases system costs. Overall, the results highlight TES as a highly valuable infrastructure for cost-efficient sector coupling in a climate-neutral European energy system.

1. Introduction

Climate-neutral energy systems that rely heavily on variable renewable energies (VRE) like wind and solar experience hourly, diurnal and seasonal differences in their electricity and heat generation [1]. In Europe, heating accounts for approximately 50% of final energy consumption, with district heating (DH) supplying around 13% of heat demand [2,3]. Thermal energy storage (TES) in combination with Power-to-Heat (P2H) offers a promising solution for the heating sector. Decarbonising this sector while integrating high shares of VRE thus represents both a significant challenge and an opportunity. This paper investigates how long-duration TES (shifting energy over periods longer than one day) can contribute to sector-coupling and flexibility in European DH networks by 2050. We focus on 2050 as the target year for climate-neutrality under the European Green Deal [4], and analyse the entire EU to capture cross-border electricity trade, which has a noticeable effect on electricity prices, and diverse DH characteristics based on their local potential for renewable heat generation.

In Europe, electricity generation from photovoltaics (PV) peaks in summer [5], while electricity generation from wind usually peaks in winter [6]. Decarbonising the heating sector relies strongly on direct electrification, mainly via heat pumps [7]. This will lead to a shift in the seasonality of electricity demand towards the heating season [8]. To balance this variation, climate-neutral energy systems require flexibility [9–11]. While there are several options providing short-term flexibility, fewer options for long-duration storage exist (i.e. several weeks or months) [12]. TES have the advantage of relatively low capital expenditures (CAPEX), high technology readiness and lower conversion losses than hydrogen storage [13].

TES technologies include tank thermal storage (TTES) and pit thermal storage (PTES) as well as ground-based solutions such as borehole thermal energy storage (BTES) and aquifer thermal energy storage (ATES). This paper focuses on TTES and PTES as the most technically mature and geographically flexible options [14–17]. Several studies have analysed the transformation of the building sector and DH grids towards climate neutrality on an international [7,18–20], national [21], or district level [22–25]. Their results show that while several forms of renewable DH generation, such as geothermal, solar thermal and biomass will play a role, the main driver of decarbonisation will come from the electrification of DH, mostly via P2H, i.e. large-scale heat pumps and electric heaters. Therefore, P2H is a key to facilitating VRE integration and reducing system costs, as shown by studies with energy

* Corresponding author. Fraunhofer Institute for Systems and Innovation Research ISI, Breslauer Strasse 48, 76139, Karlsruhe, Germany
E-mail address: alexander.burkhardt@isi.fraunhofer.de (A. Burkhardt).

https://doi.org/10.1016/j.energy.2026.141177
Received 17 December 2025; Received in revised form 22 April 2026; Accepted 26 April 2026
Available online 27 April 2026

system models (ESM) [26–28]. A meta-analysis on P2H confirms that it enhances system flexibility, facilitates VRE integration, and reduces curtailment and system costs [26]. Therefore the future success of TES depends on its combination with P2H [29]. TES increases the ability of P2H technologies to integrate VRE by storing heat when electricity prices are low and avoiding DH generation when electricity prices are high [30]. This could avoid the use of expensive hydrogen or its derivatives [31,32] to cover seasonal shifts in demand.

Very few multi-sector and EU- or country-wide ESM explicitly consider TES in DH. Of the studies that do incorporate PTES or a generic TES technology, most assume a static efficiency ranging from 90% [22] to 80% [33] or 70% [21]. The geographic coverage and spatial resolution of these studies vary significantly, but TES operation in these studies is mostly seasonal. DH-specific models often model efficiency (i.e., the self-discharge rate) dynamically in relation to the temperature or energy content of the storage [34–37], which has implications for the results: Longer storage duration correlates with higher losses, and thus lower efficiency [38], but also vice versa: higher losses over time lead to shorter storage duration [39]. Therefore, how TES losses are modelled has significant implications for the results, especially regarding TES usage patterns and their interactions with DH generation. Additionally, best practices for modelling long-term storage highlight the importance of high temporal and spatial resolution [39]. Schauß et al. [40] integrate PTES into the sector-coupled ESM PyPSA-DE using a similar approach and data to our paper [41]. They also include an estimation of the PTES potential. They varied both the self-discharge rate and CAPEX of the PTES in a sensitivity analysis. The results show that PTES increases DH generation by electric heaters and heat pumps at times of low electricity prices [41]. While PyPSA-DE focuses on Germany, our paper expands its scope to Europe. This way we capture the interactions between VRE electricity generation across Europe, P2H technologies and TES in DH and cross-border electricity trade between countries.

The methodological contribution of this paper is the integration of tank thermal energy storage (TTES) and pit thermal energy storage (PTES) with dynamic self-discharge modelling in the sector-coupled European energy system model *Enertile*. Unlike most existing studies that apply static round-trip efficiencies (typically 70-90%) [21,22,33], we model thermal losses proportionally to the state of charge (SOC), accurately capturing the physical reality that losses accumulate continuously over storage duration. This refinement is critical for accurately assessing the trade-off between flexibility value and thermal losses. We expect this to lead to a more short-term operation of TES (e.g. monthly compared to seasonal operation).

As for the analytical contribution, we quantify the system-level impacts of TES deployment across Europe with high spatial resolution (30 model regions × 4 distinct DH type networks), analysing the effects on: (1) DH generation mix and installed capacity, (2) sector coupling and variable renewable energy (VRE) integration (curtailment reduction, price-responsive dispatch patterns), and (3) total system costs and district heating generation costs. Our analysis captures the cross-border electricity trade effects and DH heterogeneity that single-country or technology-focused studies cannot reveal. Our paper addresses three interconnected research questions: (1) What role does long-duration TES play in cost-optimal climate-neutral European DH systems by 2050? (2) How does TES contribute to sector coupling, providing flexibility, and integrating VRE in the overall energy system? (3) What impacts does TES have on DH generation costs compared to systems without such storage? A greenfield 2050 perfect-foresight optimisation is the appropriate design for these questions because it isolates the system-optimal value of TES. Targeting 2050 ensures that cost and technology assumptions reflect the climate-neutral endpoint rather than near-term transition constraints.

The paper is structured as follows: Section 2 describes the methodology and data used, including the Enertile model, TES modelling, and key assumptions. Section 3 presents the results of the scenario analysis and shows how introducing TES changes the energy system by unlocking the flexibility potential of P2H technologies. Section 4 discusses the results and key limitations. Section 5 draws conclusions and outlines future research.

2. Methodology and data

To address our three research questions, we employ the sector-coupled ESM *Enertile* and improve TES modelling within the model. *Enertile* is especially suitable since, on the one hand, it has a broad scope, modelling all EU member states plus the UK, Norway and Switzerland, enabling complete representation of the European electricity market. On the other hand, it models DH generation in detail integrating high-resolution renewable and excess heat potentials through *DH type networks*.[1] The paper thus employs a deterministic optimisation approach and uses no inferential statistics, confidence intervals, or hypothesis testing. Section 2.1 describes the *Enertile* model in general, followed by details on how TES and its losses are modelled as well as the scenario design for the present analysis. Section 2.2 presents important assumptions and input data.

2.1. Enertile model and scenarios

Enertile is purely a linear optimisation model with a high level of technological, temporal and spatial detail that covers all of Europe. The energy carriers that are co-optimised are electricity, heat in DH grids, and hydrogen [27]. The model has an hourly resolution, and the key constraint of the optimisation requires that the hourly demand for those energy carriers is met in each region and each hour [31]. Fig. 1 illustrates the model and shows the interactions between electricity, DH and hydrogen. *Enertile* simultaneously minimises the cost of generation, transmission, capacity extension and storage of these energy carriers [42].

The model follows a greenfield optimisation approach for the target year 2050: it simultaneously determines the cost-optimal investment in generation, storage, and transmission capacity, as well as hourly dispatch, assuming perfect foresight over the entire year. *Enertile* has an hourly resolution and models all 8760 h of the year. This setup represents a system-optimal planning perspective suitable for assessing the value of flexibility options such as TES. The model does not simulate market dynamics, investment uncertainty, or path-dependent transition constraints. All scenarios share identical exogenous demand projections, fuel prices and technology cost assumptions (cf. Section 2.2), differing only in TES availability. This design enables us to analyse the isolated impact of TES on the overall energy system from an optimisation perspective. *Enertile* covers fixed costs for capacity expansion, and variable costs for hourly operation, which are minimised from a system perspective. The objective function minimises all costs associated with the vectors of the decision variables for installed capacity $\vec{X}$ and generation $\vec{x}$ of all energy carriers. Equation (1) shows an excerpt and simplified version of the objective function of the linear optimisation model (based on [43]).

$$\min_{\vec{x},\vec{X}} \Big[\mathrm{cost}^{\mathrm{fix}}_{\mathrm{el}}\left(\vec{X}\right) + \mathrm{cost}^{\mathrm{var}}_{\mathrm{el}}(\vec{x}) + \mathrm{cost}^{\mathrm{fix}}_{\mathrm{heat}}\left(\vec{X}\right) + \mathrm{cost}^{\mathrm{var}}_{\mathrm{heat}}(\vec{x}) + \mathrm{cost}^{\mathrm{var}}_{\mathrm{el\_chp}}(\vec{x}) + \mathrm{cost}^{\mathrm{fix}}_{\mathrm{H2}}\left(\vec{X}\right) + \mathrm{cost}^{\mathrm{var}}_{\mathrm{H2}}(\vec{x}) \Big] \quad (1)$$

with:

$\mathrm{cost}^{\mathrm{fix}}_{\mathrm{el}}$: Fixed costs of electricity capacity expansion in €
$\mathrm{cost}^{\mathrm{var}}_{\mathrm{el}}$: Variable costs of electricity generation in €
$\mathrm{cost}^{\mathrm{fix}}_{\mathrm{heat}}$: Fixed costs of capacity expansion in heat grids in €

[1] A more detailed definition of this and other technical terms can be found in Table A1 in the appendix.

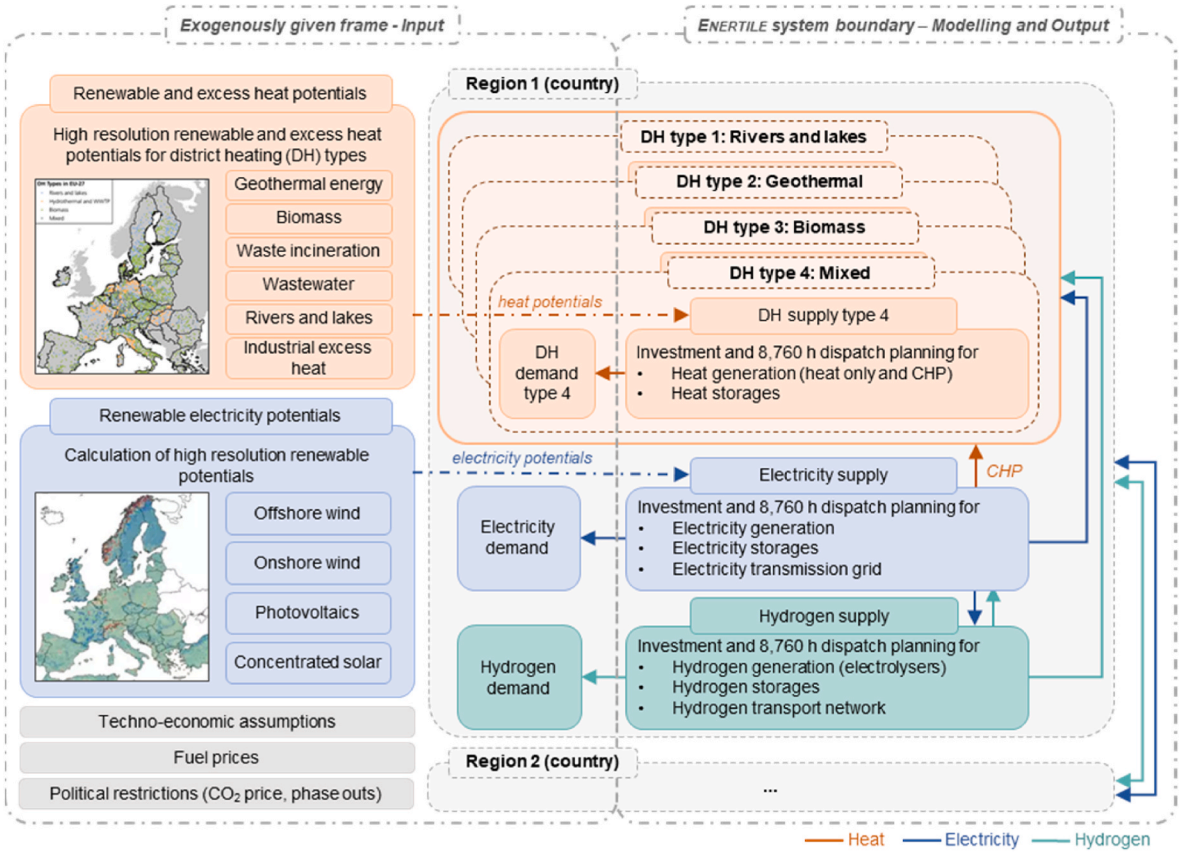

Fig. 1. Schematic overview of the Enertile model with a focus on DH (based on [19]).

$\text{cost}^{\text{var}}_{\text{heat}}$: Variable costs of heat generation in heat grids in €
$\text{cost}^{\text{var}}_{\text{el\_chp}}$: Variable costs of electricity generation from CHP plants in heating grids in €
$\text{cost}^{\text{fix}}_{\text{H2}}$: Fixed costs of hydrogen capacity expansion in €
$\text{cost}^{\text{var}}_{\text{H2}}$: Variable costs of hydrogen generation in €

The optimisation is performed using a barrier algorithm. The solver, its version, and the optimisation parameters are listed in the appendix (cf. Table A3).

2.1.1. *Renewable generation potentials and technologies*

One pre-processing step prior to the optimisation in *Enertile* is a detailed assessment of renewable electricity generation potentials, whereby potential curves on tiles measuring 7 km by 7 km are calculated. Weather data, land-availability restrictions and data on land-use and technologies for power generation are considered for each tile. Tiles are aggregated to the country level, so that each model region is represented by one node. Each tile is uniquely assigned to the country that covers the largest share of its area. This enables the model to account for wind and solar capacity across all European countries in great detail [31]. We use the single weather year 2010 for all temperature-related inputs and time series construction, based on [44]. The renewable generation potential for wind and PV is included in the optimisation in the form of maximum generation limits for wind onshore and offshore, rooftop photovoltaic (PV), utility-scale PV and concentrated solar power (CSP). Furthermore, the model includes other renewable power plants (hydro and geothermal), conventional power plants, combined heat and power (CHP) generation, batteries and a cross-border electricity transmission grid for spatial balancing. For electricity, the renewable generation from 2019 [45] is assumed as a minimum constraint in the optimisation. It is also assumed that electricity generation from hydro and geothermal energy remains unchanged until 2050.

A second component of the potential calculation as input to the *Enertile* model is the extensive potential analysis of renewable energy and excess heat resources for future DH areas across the entire EU ([19], data from Ref. [46]). Several datasets were used together with spatial matching to identify renewable and excess heat potentials for 5815 future DH areas across Europe [30]. These were then clustered using an agglomerative clustering algorithm to derive four distinct DH type networks [19,46]. The four types are each named after the renewable heat source that is especially prevalent in this DH area. The four types are: DH type 1: Rivers and lakes, DH type 2: Geothermal, DH type 3: Biomass, and DH type 4: Mixed. The allocation of the DH type networks can be found in the appendix (cf. Figure A1). Even though one source may be prevalent, each DH type network represents a multivalent heat grid with different options for DH generation, including deep geothermal, solar thermal, biogas CHP, biomass CHP and boilers, hydrogen CHP and boilers, waste incineration CHP, industrial excess heat, and heat pumps with different ambient heat sources (wastewater, rivers and lakes, ambient air). For heat extraction from the air, hourly national average air temperatures are used. Similarly, river and lake heat pumps rely on the hourly average water temperatures per country based on Manz et al. [46].[2] Since wastewater temperature is relatively stable and remains around 10 °C even in winter, we assume a constant coefficient of performance (COP) for wastewater heat pumps [19]. Biomass and waste utilisation in DH generation is limited by maximum

[2] Consistent with Manz et al. [46] we do not consider the environmental impacts of heat extraction from rivers and lakes. It is expected that the environmental impact is smaller than that of conventional power plants. Rivers with low flow rates are excluded because of remaining environmental concerns and unsuitable temperatures.

generation limits. Heat generation from deep geothermal energy and solar thermal energy is predefined exogenously by country and year and underpinned with an hourly generation profile. For hydrogen supply, the model covers electrolyser technologies, hydrogen storage and hydrogen transport pipelines [31,32]. No minimum or maximum generation limits are implemented for hydrogen. The general assumptions and constraints for the optimisation are listed in the appendix (cf. Table A6).

2.1.2. Integrating thermal energy storage

There are several ways to store thermal energy effectively. According to Ref. [14], there are three main categories: (1) sensible heat storage, (2) latent heat storage and (3) thermochemical heat storage. Sensible heat storage includes tanks (TTES) and pits (PTES). The pits are typically cone-shaped excavations filled with water as a storage medium. The sides and bottom of the pit are insulated and the top is a floating lid made from a strongly insulating material [44]. TTES and PTES can be considered the most technically mature technologies for use in DH systems [45]. Our paper extended the *Enertile* model to include PTES and TTES. Both technologies have well established parameters and there is operation data openly available [47,48]. They also do not rely on any specific geological conditions [49] beyond sufficient ground stability. Additionally, recent pilot projects with the specific aim of enhancing renewable heat uptake in DH grids have demonstrated that PTES and TTES are suited for this application [15] and justify their inclusion in the *Enertile* model.

The self-discharge rate is an important factor when modelling long-term thermal storage. Its relevance for the levelized cost of storage (LCOS) has been demonstrated by a quantitative evaluation of different storage technologies. As including self-discharge shifts the economic ranking of storage technologies, the authors propose integrating it into the LCOS index for comparing storage technologies [50]. Detailed, sector-specific DH models often model this parameter dynamically in relation to the temperature or energy content of the storage [34–37], whereas broader sector-coupled ESM often rely on a static efficiency (e.g. 70%) that is applied when the storage is discharged [21,22,33,51–53], apart from PyPSA-DE [41] and REMoD [54], which, however, both have a national focus. Our paper expands this approach to Europe. An exploratory analysis using the *Enertile* model showed that changing self-discharge rates affects the overall system results and TES operation: Lower self-discharge rates enable longer storage durations and higher heat pump shares in DH networks, while higher self-discharge rates drive short-cycle dispatch and lower TES efficiency [39]. Therefore, modelling the self-discharge rate dynamically over time in relation to the energy content seems to be the most accurate method. We draw on the values of the Danish Energy Agency dataset [55] for both TTES and PTES, and apply the self-discharge rate dynamically to the state of charge of the TES. This single loss-parameter, which represents an average case, is a reasonable simplification in ESM. In practice, losses depend on the geometry and materials of the storage, as well as ambient conditions and other factors. Both the inputs and the results are in line with the real-world data from the PTES in Dronninglund, Denmark [47].

We apply these values to the DH generation function in *Enertile*, which ensures that DH demand in each region and each DH type is met in every hour. Generation can be provided by the different DH generation technologies (Gen_i) as described above or from the storage. The storage is charged whenever DH generation is greater than DH demand. Equation (2) describes how storage losses (λ) are applied here proportionally to the state of charge of the TES in that hour. If the storage is neither charged nor discharged, additional DH must be generated that is equal to the hourly self-discharge multiplied by the state of charge.

$$D_t = \sum_{i=1}^{n} Gen_{i,t} + (1-\lambda)\cdot SOC_t - SOC_{t+1} \quad (2)$$

with:

D_t: DH demand in hour t [MWh]
$Gen_{i,t}$: DH generation of DH technology i in hour t [MWh]
SOC_t: State of charge of TES in hour t [MWh]
SOC_{t+1}: State of charge of TES in hour $t+1$ [MWh]
λ: self-discharge rate of TES [h^{-1}]

A complete formulation of all constraints and formulas of TES is provided in Appendix C. In our analysis, the parameters for both TES technologies are taken from the dataset of the Danish Energy Agency [55], including investment, variable operation and maintenance (O&M) costs and standing hourly losses[3] (cf. Table 1).

Since *Enertile* models specific milestone years, it is important to fix the state of charge of the TES at the beginning and end of the year to a certain level. We chose 50%, so that the storage does not start or finish the year empty. Since the temperature of sensible TES decreases over time, they usually require a temperature boost to reach the required temperature level of the DH grid after discharging. This is not considered here explicitly. However, since the storage is never the sole source of DH generation at any moment in time, it can be assumed that any required temperature boost comes from the other heat sources in the generation mix in that hour.

2.1.3. Scenario design

To capture the effects of TES in a climate-neutral European energy system, a baseline scenario is calculated where no TES can be built (called "***No TES***"). Additionally, two scenarios are modelled: A ***"TTES"*** scenario where only TTES can be installed, and a "***PTES"*** scenario where only PTES can be installed. We also calculated a **Mix** scenario with TTES and PTES, but the results show only investment in PTES, not in TTES. Therefore, it is not included in the results section. Furthermore, we calculated six sensitivities based on the **Mix** scenario, which also show no investment in TTES. The results from the **Mix** scenario and all sensitivities are shown in the appendix (cf. Table B2).

2.2. Data and assumptions

This section presents the underlying data and assumptions in the scenario parametrization. The year considered in this analysis is the milestone year 2050, when climate-neutrality is achieved in all scenarios and in all sectors (i.e., also in transport and industry). To achieve this goal, a CO_2 price of 500 €/t is projected for the year 2050. A uniform interest rate of 2% is assumed for all technologies. The TES options vary in their availability depending on the scenario design, while the other assumptions remain unchanged across all scenarios. A full set of assumptions is available in Appendix A – Inputs and Assumptions. This scenario setup makes it possible to account and interpret changes in the energy system induced by TES. The techno-economic assumptions for investment options in *Enertile* (besides TES) are listed in the appendix (cf. Table A2). The optimal investment and operation of the different technologies depend on the assumed energy carrier prices, which are outlined in Table A4 in the appendix.

The demand for electricity, hydrogen and DH is defined exogenously and entered in the *Enertile* model (cf. Fig. 1 in Section 2.1). Demand data for electricity and hydrogen are taken from the *Elec_60* scenario in Ref. [56] based on the project "Potentials and levels of electrification of space heating in buildings" (ENER C1 2019-481). In this scenario, the heat demand of decentralised heat pumps in buildings amounts to 708 TWh, the total electricity demand of all other sectors reaches 3463 TWh

[3] For PTES this parameter is calculated from "Energy losses during storage [K/day]" by dividing by 24 h of the day and converted into %/day by dividing through the assumed temperature spread of the PTES. We use the 2050 "crtl" scenario for all inputs [42]. For TTES, the parameter is shown in % loss per day, which is divided by 24 h of the day. It is then applied as a factor on the state of charge of the storage (cf. Equation (2)).

Table 1
Techno-economic parameters of TES options in 2050 used in Enertile.

Technology/ parameters	Investment (€/kWh)	Variable O&M (€/MWh)	Lifetime (yr.)	Standing hourly losses λ (relative to TES SOC)	Source
TTES	3.0	8.81	40	0.0000774	3,000m^3, sheet *141 Large hot water tank in* [55]
PTES	0.9	2.50	30	0.0000606	70,000m^3, sheet *140 PTES seasonal in* [55]

and the hydrogen demand is 660 TWh in Europe in 2050.

The DH demand in Europe in 2050 is based on the HT scenario presented in Ref. [46], which also is based on the *Elec_60* scenario in Ref. [56]. DH demand amounts to 732 TWh for the whole of Europe in 2050. Compared to today's levels of DH demand in Europe around 445 TWh [57], this is an ambitious deployment assumption. However, this estimate falls within the range of other European energy system scenarios, which anticipate 325 to 800 TWh of DH demand by 2050 [58–61]. The annual DH demand is converted into an hourly profile (D_t) in *Enertile*, considering outdoor temperatures. The annual energy demands per country can be found in the appendix (cf. Table A7).

3. Results

Table 2 compares the central results for the three scenarios, to give a brief overview of the scenario dynamics. These results are explained in the following sections in more detail. The results show that the change from **No TES** to either **PTES** or **TTES** is substantive, but the results for **TTES** and **PTES** are quite similar. In the **PTES** scenario more TES capacity is installed (16.2 TWh compared to 8.6 TWh in **TTES**). A map of Europe showing the installed TES per model region can be found in the Appendix, cf. Figure B2. The storage is operated more long-term in the **PTES** scenario, which leads to bigger changes in DH generation (shift to heat pumps, away from biomass and hydrogen), which is further analysed in Section 3.1. The introduction of TES increases the installed capacity of VRE, while simultaneously reducing curtailment, which is further elaborated in Section 3.2. This reduces total system and DH costs, which is described in more detail in Section 3.3.

3.1. District heating generation mix and the impact of TES

Fig. 2 shows the resulting DH generation mix and the changes induced by introducing TES into the model. In the **No TES** scenario, biomass CHP has the highest share of DH generation with 198 TWh, followed by air-source heat pumps with 189 TWh. Hydrogen boilers contribute a low share to the DH generation mix as a back-up technology. The introduction of TES leads to a shift in the DH generation mix towards heat pumps, reducing the need for biomass CHP (reduction from 198 to 132 TWh (**TTES**) and 110 TWh (**PTES**)), and means that hydrogen boilers are no longer required. In both TES scenarios, DH curtailment is reduced by as much as 50%. The shift towards electrification is higher in the **PTES** scenario, also evident by the small increase in the use of direct electric heaters.

The full load hours (FLH), calculated as generation divided by capacity, of the air-source heat pumps and river and lake heat pumps are significantly reduced in the **TTES** and **PTES** scenarios (cf. Table 3), as both generation (cf. Fig. 2) and capacity (cf. Fig. 3) increase. This reduction in FLH reflects a shift from baseload operation to a flexible, price-responsive dispatch of heat pumps. This means heat pumps generate heat during periods with low electricity costs, with TES bridging any supply gaps. In contrast, the FLH of direct electric heaters, because TES enables them to generate DH in hours with very low electricity costs. FLH for wastewater heat pumps also increase by about 200 h, since these heat pumps have the highest COP in winter. While TES reduces the overall capacity utilization of P2H technologies, it substantially enhances system flexibility (see Section 3.2) and lowers DH generation costs (see Section 3.3).

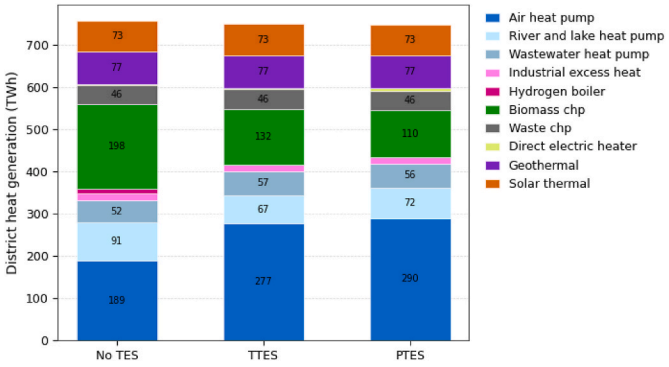

Fig. 2. DH generation by technology in the scenarios in Europe in 2050 (aggregated).

The effect of TES on the installed DH capacity is even greater than for the DH generation, as shown in Fig. 3. In the **No TES** scenario, hydrogen boilers reach high shares of the capacity (72 GW_{th}), underlining their role as back-up technology. Biomass (55 GW_{th}) and waste CHP (46 GW_{th}) also provide dispatchable capacity. In the **TTES** and **PTES** scenario, no hydrogen boilers are built, and biomass CHP capacity is also reduced to 34 and 27 GW_{th} respectively. At the same time, the capacity of heat pumps increases significantly, especially air-source heat pumps (210 GW_{th} in **TTES** and 213 GW_{th} **PTES**). The increased heat pump capacity in TES scenarios represents a trade-off between higher capital investment and lower operational costs: While this increases fixed costs, it reduces variable costs through cheaper electricity consumption and avoided hydrogen use, resulting in net savings (see Section 3.2).

Fig. 4 shows the DH capacities in each DH type network. Comparing the different DH type networks with each other, we see that the *DH type 2: Geothermal* is dominated by DH capacity from geothermal energy (14-15%) and waste CHP (45-49%) and has the lowest share of P2H

Table 2
Key results for Europe (aggregated) for the main scenarios.

Variable	Unit	No TES	TTES	PTES
Installed TES capacity	TWh	-	8.6	16.2
Median TES cycles per year		-	25	12
Heat pump DH generation	TWh	332.0	401.2	418.6
Biomass CHP DH generation	TWh	198.3	131.7	110.3
Hydrogen Boiler DH generation	TWh	12.4	0.0	0.0
Hydrogen Boiler DH capacity	GW_{th}	72.3	0.0	0.0
Installed VRE (wind + PV) capacity	GW_{el}	2078.1	2103.1	2114.6
Curtailment Electricity	TWh	59.5	43.1	38.9
Total system cost change vs. No TES	%	-	−1.02%	−1.30%
Average DH SMC	€/MWh	15.1	11.7	11.1

Table 3
Full load hours (FLH) of P2H technologies.

Scenario/FLH of P2H technology	Air-source heat pump FLH [h]	River and lake heat pump FLH [h]	Wastewater heat pump FLH [h]	Direct Electric Heater FLH [h]
No TES	2415	2901	1455	150
TTES	1316	1533	1624	393
PTES	1363	1396	1678	463

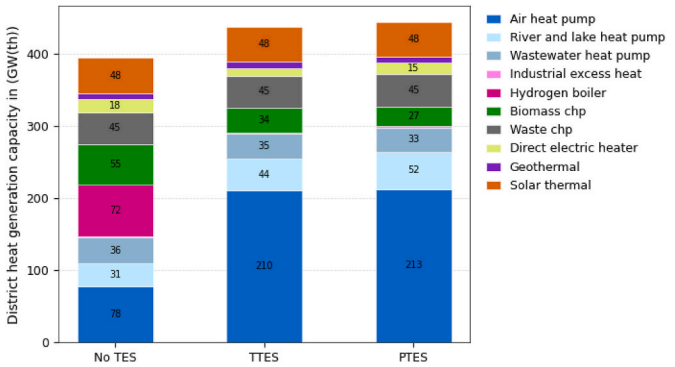

Fig. 3. DH generation capacity in the scenarios in Europe in 2050 (aggregated).

capacity. Geothermal also contributes to *DH type 1: Rivers and lakes*, but the main generation technology here is river and lake heat pumps (22% in **No TES**, 36% in **TTES,** and 44% in **PTES**). *DH type 3: Biomass* and *DH type 4: Mix* show relatively similar generation mixes. Here the introduction of TES leads to the biggest increase in generation from air-source heat pumps, from 24% to 58% in the **TTES** and to 59% in the **PTES** scenario. The variation across DH types reflects their renewable potential and demand characteristics. *DH type 2* shows a limited impact of TES due to abundant low-cost baseload geothermal energy and the high share of waste CHP, reducing the need for flexible P2H dispatch. Conversely, *DH types 3* and *4* lack abundant baseload resources, making TES-enabled flexible heat pump operation economically attractive. The high electrification in *DH type 1* reflects the combination of favourable heat pump COPs from water sources and sufficient TES capacity to optimise dispatch.

Although the overall results for TTES and PTES are quite similar, their operation differs significantly under the given assumptions. Fig. 5 shows the range of the number of cycles for each TES technology, region and DH type network. The number of cycles is calculated by dividing the discharged energy by the storage capacity. PTES have significantly lower storage cycles than TTES. On average, PTES follow a monthly cycle, whereas TTES tend towards a bi-weekly or weekly cycle. An example of this behaviour is shown for the operation of TES in Germany in Figure B1in the appendix. The overall results show that the installed TES capacity is higher for PTES, at 16.2 TWh, compared to 8.6 TWh for TTES. Comparing the different DH type grids reveals that *DH type 2: Geothermal* has the lowest number of cycles (median 18 in **TTES**, 10.2 in **PTES**), and the more heavily electrified DH type networks (i.e., *DH type 3*) have a higher number of cycles (median 29.3 in **TTES**, 17.2 in **PTES**). The SOC of TES in Germany also reveals the difference between DH type networks with the same dynamic (cf. Figure B1 in Appendix B). This shows that the value of TES is not primarily due to a seasonal shift, but due to more flexible P2H generation that is able to capitalise on cheap electricity costs. Their larger storage volumes mean that PTES can shift DH generation over longer periods than TTES.

3.2. *Contribution of TES to sector coupling and flexibility*

There are several ways in which TES, in combination with P2H, can contribute to sector coupling, e.g. by increasing the utilisation of VRE sources, by shifting electricity consumption, and by interacting with other forms of flexibility. The introduction of TES leads to higher capacities of wind onshore and PV. Compared to the **No TES** scenario, wind onshore capacity increases by 2.5% in the **PTES** scenario, and PV utility scale capacity by 2%. Fig. 6 illustrates the electricity generation mix in the three scenarios. It shows that, less biomass CHP capacity is

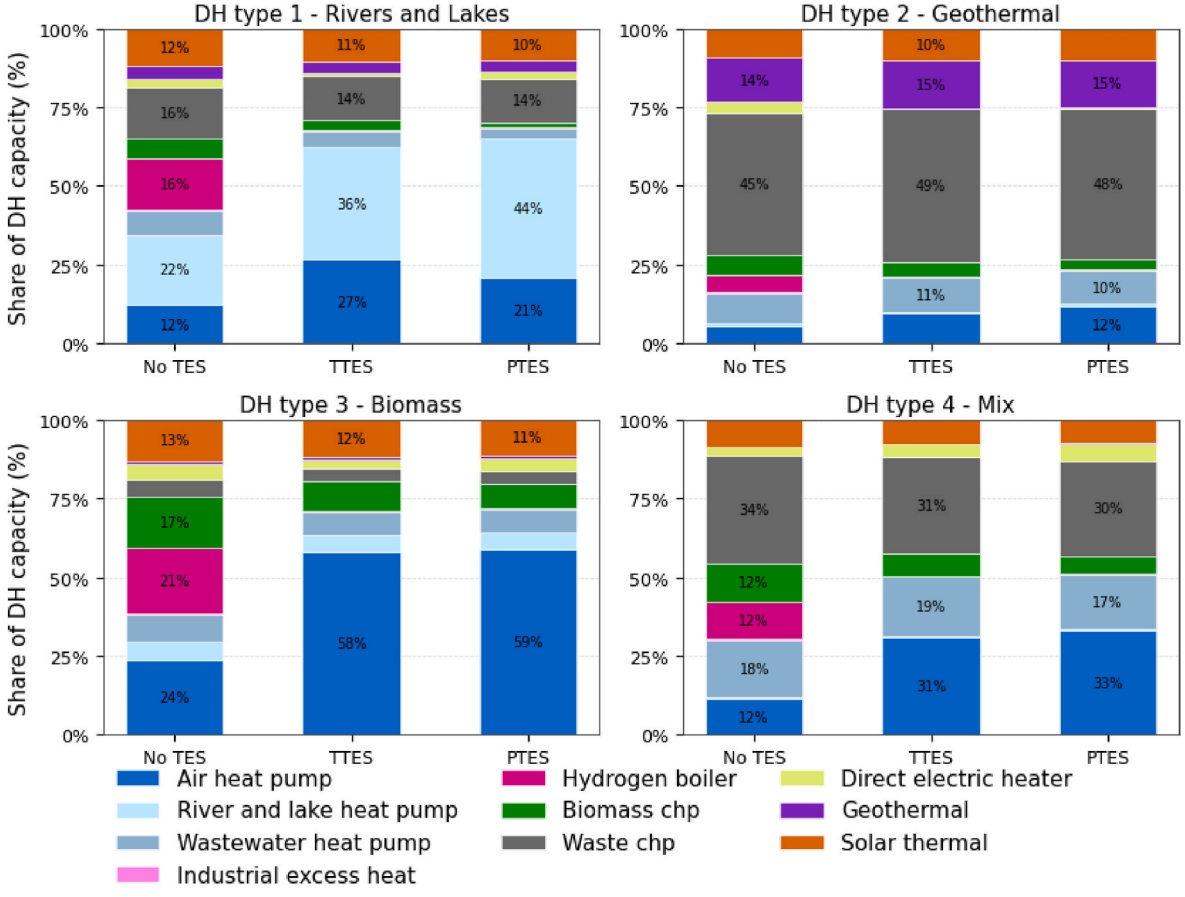

Fig. 4. Share of DH capacity by DH type networks in Europe in 2050 (aggregated).

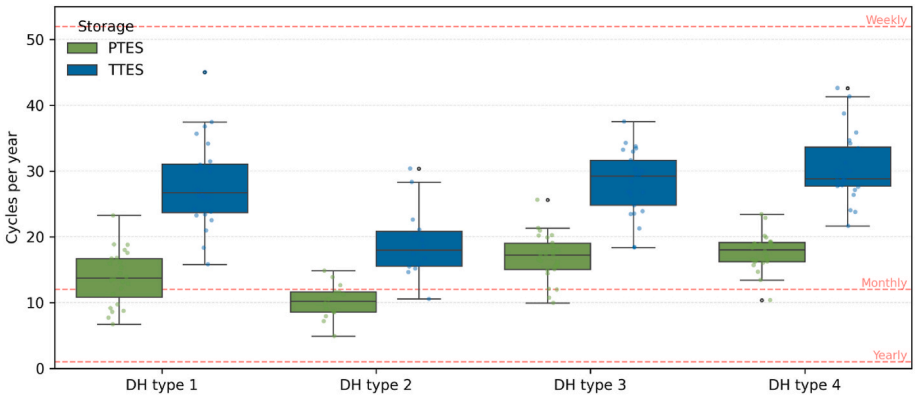

Fig. 5. Number of storage cycles by region and DH type grid (not aggregated). Note: we calculate the number of cycles as total discharged energy divided by storage capacity; box plots show median (centre line), interquartile range (box), and full range (whiskers). N = 240 [30 regions × 4 DH types × 2 scenarios]. The horizontal lines indicate the number of cycles corresponding with yearly (1), monthly (12) or weekly (52) operation.

installed in the **TTES** and **PTES** scenarios, and in turn more hydrogen backup power plants are needed (141 GW in **No TES**, 150 GW in **TTES**, 154 GW in **PTES**).

TES enables P2H technologies to shift operations towards periods with low electricity prices. Fig. 7 quantifies this shift by comparing the average electricity cost of each P2H technology to the annual average electricity price per region. The electricity costs are the short-run marginal costs (SMC) of the electricity commodity. SMC represent the cost of producing one additional unit of output in the short run (also called the dual variable). They should not be interpreted as end consumer prices but as an indicator of scarcity or abundance in the model. This indicator is widely used in many publications using ESM [21,27,33]. Positive values (shown in red) indicate that the electricity cost of P2H technologies is higher than the annual average. Negative values (shown in blue) indicate that heat pumps and direct electric heaters can shift their heat production to hours with lower electricity costs.

For the **No TES** scenario, the average cost of P2H electricity demand is higher than the average annual electricity cost. This effect is strongest for wastewater heat pumps, which are the best option because they have the highest COP during winter hours with cold temperatures and high electricity costs. Electric heaters are the P2H technology with the worst efficiency, and highest sensitivity to the electricity price. For the **TTES** and **PTES** scenarios, we observe a significant shift. TES allows electric heaters to operate primarily when electricity costs are very low. Similar effects apply to river and lake heat pumps and air-source heat pumps. Both TTES and PTES allow them to use significantly cheaper electricity. Wastewater heat pumps can also reduce their electricity cost significantly. For them, we observe the biggest jump from the **TTES** scenario to the **PTES** scenario, as the longer storage duration and higher storage capacity of PTES (discussed in Section 3.1) allow more flexible operation.

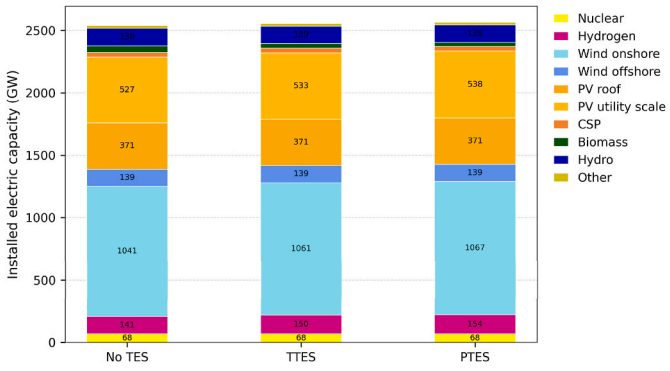

Fig. 6. Installed electric capacities of electricity generation technologies in Europe in 2050 (aggregated).

There is a significant shift in DH generation to hours with cheaper electricity costs if TES is introduced. Fig. 8 shows the respective DH generation mix for ten electricity cost deciles. Electricity cost deciles divide all the hours of a year into ten equal groups, which can be ranked from the lowest (first decile) to the highest (tenth decile) electricity costs for each region. We observe that, in the **No TES** scenario, DH generation is highest in the eighth, ninth and tenth deciles, as these are mainly dark winter days. Fig. 8 also shows that hydrogen boilers are only used in the **No TES** scenario when electricity costs are highest. The use of biomass CHP also increases with rising electricity costs. The **TTES** scenario and, to an even greater extent, the **PTES** scenario show a strong increase in DH generation, mainly from P2H technologies, in the bottom two deciles, and a strong decrease in the ninth and tenth deciles. DH generation in the first decile increases from 60 TWh in **No TES** to 128 TWh in the **TTES** and 142 TWh in the **PTES**, an increase that is mainly driven by generation from heat pumps. In the tenth decile, DH generation decreases from 137 TWh in **No TES** to 86 TWh in the **TTES** and 76 TWh in the **PTES**. These results indicate how TES can contribute to sector coupling by allowing a more flexible operation of P2H technologies and by shifting DH generation to times with cheaper generation costs (i.e., low electricity costs).

3.3. *System and district heating generation costs*

The operational changes induced by TES deployment translate to economic benefits at both the system and DH levels. Since the scenarios follow a greenfield approach, we focus on the relative change in total system costs. Allowing the model to invest in TES and keeping all other parameters the same over all three scenarios, reduces total system cost by 1.02% in the **TTES** scenario, and by 1.30% in the **PTES** scenario, compared to the **No TES** scenario. The cost reductions are achieved mainly by the change in the DH generation mix and a more efficient use of VRE sources for electricity and DH generation. Compared to the **No TES** scenario, the cost of capital in the DH sector in the **PTES** scenario increases due to additional investment in TES and heat pumps (an increase of 35% compared to **No TES**), as is shown in Fig. 9. On the other hand, operating and maintenance costs in the DH sector decrease by 19% and fuel costs decrease by 33%, compared to the **No TES** scenario. TES deployment reduces electricity curtailment by 28% (from 60 to 43 TWh in **TTES**) and 35% (from 60 to 39 TWh in **PTES**) compared to the **No TES** scenario. A certain level of curtailment remains cost-optimal, but the reduction in curtailment shows the ability of the system to absorb cheap, abundant electricity from VRE. The deeper electrification of DH is the main driver of the cost reduction, as P2H can make use of the output of wind and PV at times that are more opportune from a system perspective.

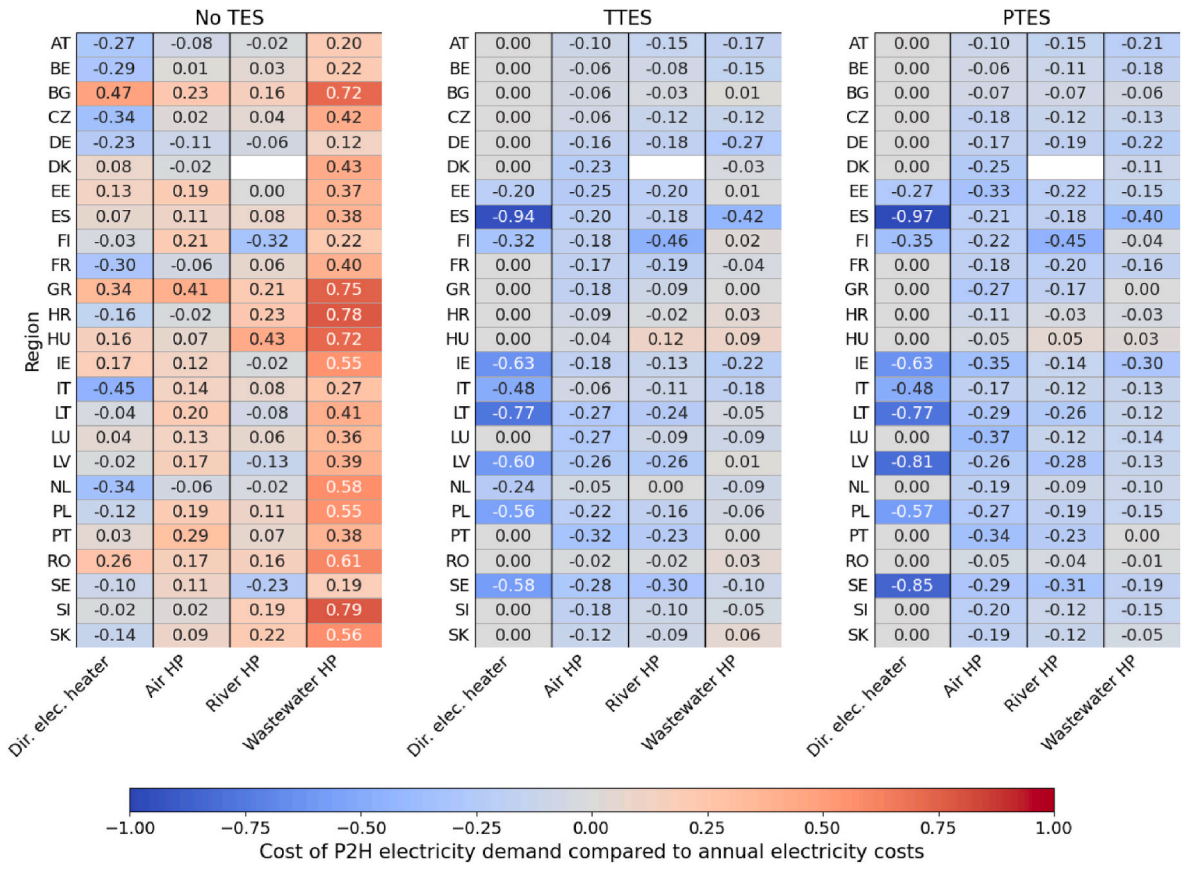

Fig. 7. Relative cost change of the electricity used for P2H technologies compared to the average annual electricity price per region across all DH type grids (aggregated).

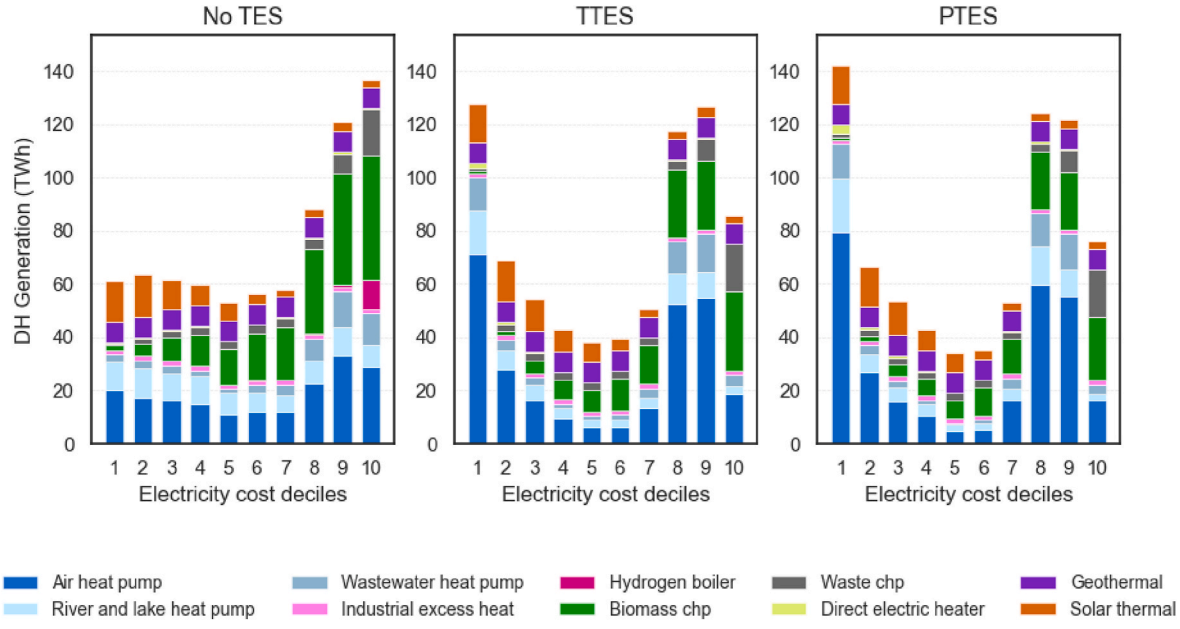

Fig. 8. DH generation mix (sum over all regions and DH type networks) by electricity cost deciles (SMC calculated for each region) for Europe in 2050.

This cost reduction due to TES can also be observed in DH generation costs. The SMC of DH generation costs are analysed for all three scenarios. Fig. 10 shows the distribution of SMC of DH generation for all regions and DH type grids over the full year without aggregation. In the **No TES** scenario, DH generation costs are mostly driven by the fuel price of the most expensive DH generation technology, which are hydrogen boilers in this scenario. The highest prices shown in Fig. 10 for the **No TES** scenario represent the use of hydrogen boilers, together with heat pumps in hours of very high electricity prices (SMC over 80 €/MWh). The high DH generation costs of using hydrogen boilers can be avoided

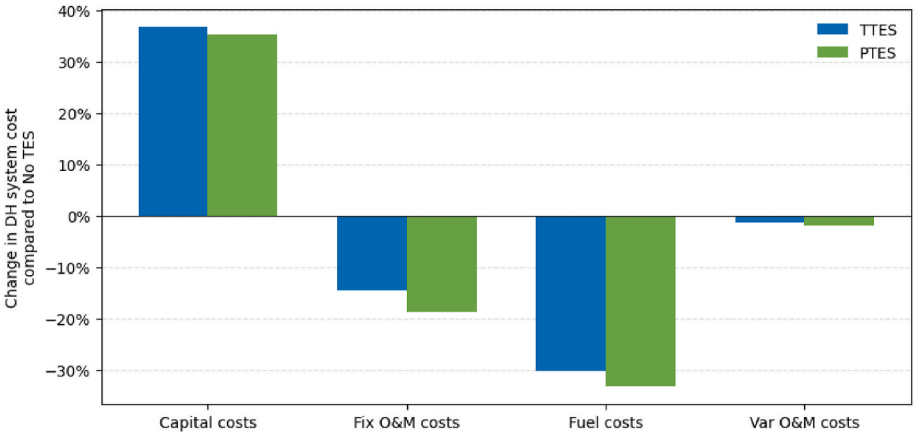

Fig. 9. Change in DH system costs compared to the No TES scenario (aggregated on European level).

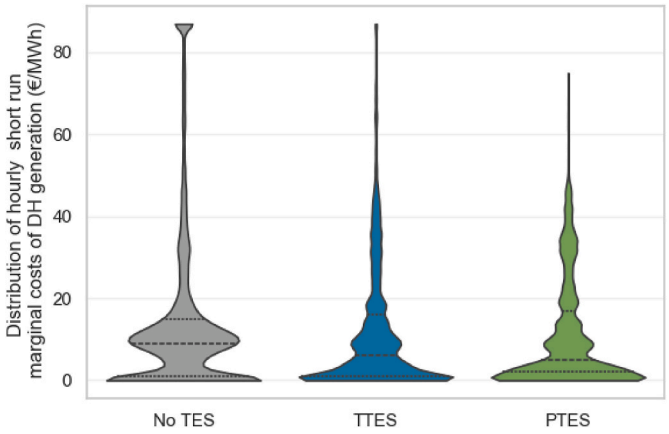

Fig. 10. Distribution of DH generation costs (SMC) for all regions and DH type grids (no aggregation across regions or DH types).

by introducing TES. Although there are still some hours with SMC of more than 80 €/MWh in the **TTES** scenario, the **PTES** scenario does not have any hour with a SMC higher than 74 €/MWh. The average SMC are 11.74 €/MWh in **TTES** and 11.08 €/MWh in **PTES**, while the average in the **No TES** scenario is 15.05 €/MWh. The median (dashed line) is also the highest in **No TES** and the lowest in **PTES**. This is mainly due to the possibility of using cheap electricity for heat pumps and electric heaters, as shown in Figs. 7 and 8.

There are varied effects regarding the interaction with other forms of flexibility. We observe slight increases in hydrogen underground storage and utility-scale batteries in the **TTES** and **PTES** scenarios compared to the **No TES** scenario. These are the result of greater electrification and VRE installation that increase the overall need for flexibility.

To strengthen the robustness of the results, a sensitivity analysis was conducted focusing on two central parameters: biomass price, as a previous paper has revealed the high price sensitivity of this parameter [19], and PTES CAPEX, as there is a high level of uncertainty regarding future CAPEX. Biomass prices were varied from 6.5€/MWh to 26€/MWh, compared to the 13€/MWh in the main scenarios (**No TES**, **TTES**, **PTES**). PTES CAPEX was increased and decreased by 25%. In the sensitivity analysis both PTES and TTES were allowed (like in the **Mix** scenario), to observe the competition between the two technologies. The sensitivity results are shown in Table B2 in the appendix. Varying the CAPEX did not significantly affect the results, although more PTES is built in the scenario with low PTES CAPEX. Across sensitivities, PTES is favoured over TTES, leading to no TTES investment. Very low biomass prices lead to a huge increase in biomass CHP generation, which in turn crowds out a proportion of the heat pump generation. At the same time, in the sensitivity with very low biomass prices, PTES investment is reduced significantly to half of its value, in the **Mix** scenario. Nevertheless, it remains cost-optimal to a certain level. Higher biomass prices fully eliminate biomass generation from the cost-optimal solution. In these cases, PTES deployment increases by 42% and air heat pump generation in DH increases by 32.7% compared to the **Mix** scenario.

4. Discussion

This paper presents a novel Europe-wide analysis of TES in a climate-neutral system with detailed spatial representation and high-resolution renewable and excess heat potentials for DH. Our main methodological contribution is the integration of dynamic self-discharge modelling, which applies losses proportionally to the state of charge rather than using static round-trip efficiencies. This refinement significantly impacts operational conclusions. Our results reveal operating patterns that contrast sharply with seasonal-storage assumptions [21,22,33], as described quantitatively in Section 3.1. The specific number of cycles may vary with different loss assumptions, multi-year weather inputs, or relaxed boundary conditions, but has important implications for the operational planning and economic assessment of TES, as it demonstrates that its value primarily stems from flexible weekly or monthly load shifting rather than purely seasonal shifting. The four DH type networks represent a substantive advance over analyses using a single aggregated DH system, since DH Type networks show different responses depending on their generation mix. A single-type representation would average these effects, obscuring both the contexts where TES delivers the highest value and the mechanism behind it.

The integration of TES enables deeper electrification of DH generation and more flexible use of P2H technologies, reducing total system and DH costs. While our findings qualitatively align with Sifnaios et al. [33] and Herpich et al. [22] regarding cost-saving potential, our dynamic loss modelling provides more realistic operational patterns and efficiency trade-offs. Our results back previous research highlighting the cost-saving potential of flexibility provided by P2H [26–28,62,63]. Both TTES and PTES are technically mature technologies with proven real-world operation [48]. PTES achieves greater system cost savings primarily due to its lower capital costs and longer storage duration, enabling more effective load shifting. However, practical deployment considerations include space requirements, which are not covered in this paper. PTES requires significant ground area, which may be challenging in dense urban areas, while TTES can be built vertically, offering advantages in space-constrained locations. Neither technology requires specific geological conditions beyond sufficient ground stability [14], making them more geographically flexible than BTES or ATES. Options like BTES and ATES could play roles in specific contexts but require

suitable underground geology. Comprehensive European-wide potential assessments for these technologies are not yet available. A detailed spatial suitability assessment would support implementation planning for all TES and should be explored in future research.

As shown in the results, TES substantially reduces biomass reliance and eliminates hydrogen boilers from the cost-optimal DH mix (cf. Figs. 2 and 3), with the implications for competing sectoral demands. Both fuels face constraints in terms of availability and competing sectoral demands. Given that sustainable biomass is limited and has air quality impacts, policies restricting biomass use would further strengthen the case for TES. Our results further suggest that TES complements, rather than replaces, other flexibility options. We observe slight increases in hydrogen underground storage and batteries in TES scenarios, driven by higher VRE capacities and deeper electrification.

Our modelling approach has several methodological limitations that should be acknowledged. Firstly, our greenfield 2050 optimisation with perfect foresight provides a system-optimal planning perspective and quantifies the value of TES under ideal coordination. However, it does not capture market-based investment decisions, uncertainties (e.g. regulatory or cost-based), financing heterogeneity or transition path dependencies. Secondly, *Enertile* does not explicitly model supply/return temperatures in DH grids or the temperature boost potentially required after TES discharge. We assume that the concurrent operation of other DH generators provides the necessary temperature augmentation. This simplification, while appropriate for European-scale energy system modelling and consistent with standard practice [21,22,33], should be refined in regional or site-specific studies. Thirdly, our dynamic self-discharge modelling uses a single loss parameter proportional to the SOC, based on Danish Energy Agency data [55] and validated against Dronninglund PTES operation [48]. While this represents a significant improvement over static efficiency assumptions, real-world losses depend on geometry, materials, temperature gradients, and ambient conditions. Site-specific conditions introduce variation around our mid-range assumptions but should be explored in future research. Fourthly, our fixed 50% SOC boundary condition at the start and end of the year affects seasonal storage incentives. Relaxing this constraint could change PTES utilisation at the beginning and end of the year. We model only one weather year, which may affect the cycling results, and storage demands. Spatial siting assessments, particularly for land-use requirements of PTES, represent a valuable next step for translating our European-scale findings into site-specific implementation plans. Finally, incorporating non-CO_2 environmental co-benefits and impacts, such as effects on aquatic ecosystems from river and lake heat extraction, would further enrich the sustainability assessment of large-scale TES deployment. Moreover, we kept the DH share of heating demand constant and fix the geothermal and solar thermal output across scenarios. While this approach isolates the impact of TES, it does not assess whether TES increases the cost-optimal share of DH versus decentralised solutions (mainly decentralised heat pumps), which is a promising direction for future work given the substantial cost reductions observed.

Besides these limitations, real-world deployment commonly encounters barriers beyond technological and economic optimisation. These include regulatory challenges, market design issues, the need for coordination between multiple stakeholders, and potential land-use conflicts. Despite these challenges for near-term implementation, our greenfield approach provides a vision of long-term system-optimal design. Thus, policies to address these challenges should be considered, as our results show a robust long-term benefit from TES.

Despite these limitations, our results demonstrate that TES is highly valuable infrastructure for cost-efficient sector coupling in a climate-neutral European energy system. It provides a robust foundation for policy development and regional implementation studies. Future research could prioritise the following aspects: (1) a systematic comparison of TES technologies (TTES, PTES, BTES and ATES) in relation to geological and spatial constraints; (2) relaxed boundary conditions and multi-year optimisation to assess the trade-offs between truly seasonal and monthly storage; (3) a systematic comparison of dynamic vs. static loss modelling of energy storage technologies, (4) combination with dynamic DH temperature modelling; and (5) an analysis of the impact of TES on the cost-optimal deployment of DH versus decentralised heating solutions.

5. Conclusion

Integrating variable renewable electricity while meeting seasonal heat demand is a prerequisite for climate-neutral district heating (DH) systems. Our paper aims to quantify the system-level role of large-scale thermal energy storage (TES) in enabling cost-effective decarbonisation of DH across the EU by the year 2050. The existing *Enertile* energy system model is enhanced through the integration of tank thermal storage (TTES) and pit thermal storage (PTES) with dynamic self-discharge modelling. This approach considers losses proportional to the state of charge rather than as static round-trip efficiencies. This refinement captures the critical trade-off between storage duration and thermal losses, revealing operational patterns that differ from those studies assuming a static efficiency.

Our analysis yields three key findings. Firstly, TES enables deeper DH electrification: PTES deployment increases heat pump generation in DH from 332 to 418 TWh compared to scenarios without storage. TES reduces biomass use in DH generation by up to 45%. Hydrogen boilers, which serve as expensive backup generation in the No TES scenario, are eliminated in both TES scenarios. This overall shift toward electrification reduces dependence on scarce, sustainable biomass and costly hydrogen, which are subject to competing demands from harder-to-decarbonise sectors. Contrary to studies using static efficiency assumptions, the PTES in our study operate in predominantly monthly cycles (cf. Fig. 5). Secondly, TES facilitates sector coupling and VRE integration by enabling flexible Power-to-Heat (P2H) dispatch, shifting DH generation towards hours with low-electricity costs. This reduces electricity curtailment and supports additional VRE capacity deployment. Thirdly, TES provides system-wide benefits: The total system costs decrease by 1.02% in the **TTES** scenario and by 1.30% in the **PTES** scenario, and DH generation costs are also reduced. These benefits are robust to variations in PTES investment expenditures. If biomass becomes significantly cheaper, TES deployment and electrification are reduced, but the overall effects remain stable (cf. Table B2).

Our greenfield optimisation framework quantifies the system-optimal end-state under perfect foresight and 2050 cost assumptions but does not model transition pathways, market design barriers, or additional constraints such as land availability, existing infrastructure lock-in, regulatory hurdles, or public acceptance. Actual deployment trajectories will depend on policy and site-specific engineering considerations beyond the scope of this paper. The results are also conditional on the loss parameters assumed, the simplified temperature modelling and our overall model assumptions.

Nevertheless, our results clearly indicate that TES should not be regarded as merely a supplement to DH generation; rather, it is an enabling infrastructure for cost-effective deep decarbonisation. Future research could explore other TES technologies, such as ATES and BTES, refining the modelling of temperatures in DH grids, or analyse the interaction between different long-term storage technologies. Such future research initiatives could expand upon our methodological

approach and findings.

CRediT authorship contribution statement

Alexander Burkhardt: Writing – original draft, Visualization, Software, Methodology, Investigation, Formal analysis, Data curation, Conceptualization. **Miriam Frömel:** Writing – original draft, Software, Methodology, Data curation. **Gerda Deac:** Writing – review & editing, Validation, Software. **Anna Billerbeck:** Writing – review & editing, Validation, Supervision, Conceptualization.

Declaration of AI and AI-assisted technologies in the writing process

During the preparation of this work, the authors used "deepL translator', "Grammarly" and "ChatGPT" to correct potential grammar mistakes and improve readability. After using this tool/service, the authors reviewed and edited the content as needed and take full responsibility for the content of the publication.

Declaration of competing interest

The authors declare that they have no known competing financial interests or personal relationships that could have appeared to influence the work reported in this paper.

Acknowledgements

The authors acknowledge funding from the German Federal Ministry of Research, Technology and Space (Ariadne project FKZ 03SFK5D0-2).

Appendix A. Inputs and Assumptions

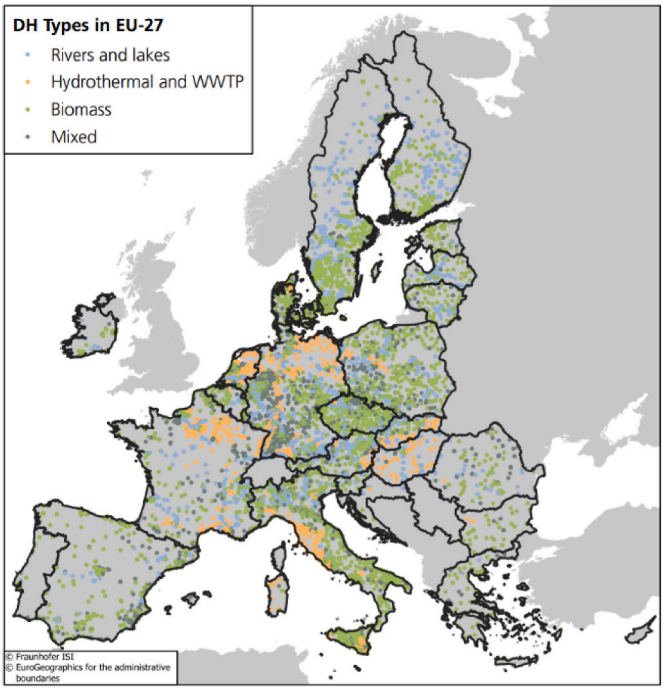

Fig. A1. Distribution of DH types across the EU for the RES_HT scenario [46].

Table A1
Notation and definition table

Notation	Definition
State of charge (SOC)	The SOC, in absolute terms, is the energy stored in the TES in each model region and DH grid. It can also be calculated as a relative value by dividing it by the maximum TES capacity in each model region an DH grid.
Short-run marginal costs (SMC)	SMC are defined as the additional cost which is required to produce on more unit of energy. These are represented by the dual variable of the demand-supply equation, and are a central output from the *Enertile* model
Electricity costs	These are the SMCs of the electricity variable in the *Enertile* model for each model region. Since *Enertile* takes a central planner's perspective, these costs should not be interpreted as final consumer costs, but rather as generation costs of electricity at any given hour.
DH type grid	DH type grids are aggregations of single DH grids based on a certain criterion, to reduce modelling complexity. Commonly used criteria are the temperature level [18] of the grid or the size of the supplied municipality [33]. In *Enertile*, we cluster and aggregate DH grids by their renewable heat generation potential. For more details refer to Ref. [19].

Table A2
Techno-economic parameters of investment options in 2050 from Ref. [64] used in Enertile

Technology		Investment (€/kWh)	Fixed O&M (€/kW)	Variable O&M (€/MWh)	Lifetime (a)	Efficiency el (chp)	Efficiency heat (or H2)
Electricity	Battery storage	204	5.5	0.0	10	95%	
	Combined cycle hydrogen turbine	750	11.3	3.0	30	61%	
	Hydrogen turbine	400	7.5	1.5	30	41%	
CHP	Biomass CHP	2900	103	2.1	25	30% (71%)	
	Waste to energy CHP	6460	148	23.6	25	24% (80%)	
	Hydrogen CHP	950	30	3	30	48% (88%)	
DH	Biomass boiler	750	42.9	0.7	25		103%
	Electric boiler	60	0.9	0.4	20		99%
	Air source heat pump	760	2.0	1.7	25		variable
	River and lake heat pump	380	4.0	1.7	25		variable
	Wastewater heat pump	570	2.0	1.7	25		variable
	Geothermal	1300	18.8	2	30		-
	Solar thermal	310	60	0	30		-
	Industrial excess heat	1500	80	5.6	25		-
Hydrogen	Hydrogen boiler	50	1.7	0.9	25		104%
	Storage (salt caverns)	0.55	0.2	0	40		100%

Note: All cost data is in €2020.

Table A3
Solver specification and optimisation settings[4]

Parameter	Specification
Solver	Gurobi
Optimizer version	11.0.1. build v11.0.1rc0
Method	2
TimeLimit	432000 s
FeasibilityTol	1e-07
BarIterLimit	10000
BarConvTol	1e-06
BarHomogeneous	1
Crossover	0
IISMethod	1
NumericFocus	1
Presolve	1

[4] Parameter names as specified in Ref. [65]. Parameters that are not mentioned in the Table are set to their default values.

Table A4
Fuel price assumptions (€/MWh)

	Biomass	Gas	Hard coal	Lignite	Nuclear	Oil
Fuel price	13	31.44	12.13	3.749	3.11	65.29

Table A5
Assumed hydrogen import costs from non-EU countries

	Import costs (€/MWh_{H2})	Infrastructure Investment[5] (€/kW_{H2})	Fix O&M (€/kW_{H2})	Lifetime (a)
Import by ship	80.20	875	2.5	30

[5] Increased capacity price on imports compared to Ref. [66], to better capture seasonality of imports and need for hydrogen storage along the supply chain.

Table A6
General assumptions and aggregated constraints for capacity expansion and generation (Note: Hydrogen production in Europe is modelled endogenously. Hence, there are no general assumptions and constrains for electrolysis. Besides, hydrogen can be imported outside of Europe. Import prices are shown in Table A5)

	Parameter	Type of constraint			
		Equal	Minimum	Maximum	Unit
general	interest rate	2%	-	-	%
	CO2 price	500	-	-	€/t
electricity	biomass (turbine + chp)	-	9.557	113.664	MW_{el}
	wind onshore	-	160.329,80	2.520.191	MW_{el}
	wind offshore	-	18.732	2.520.380	MW_{el}
	PV (rooftop + utility scale)	-	114.680	-	MW_{el}
	rooftop PV	-	-	1.364.085	MW_{el}
	utility scale PV	-	-	2.447.211	MW_{el}
	concentration solar power	-	2.314	781.424	MW_{el}
	hydro	139.006	-	-	MW_{el}
district heating	waste chp	-	46.085	92.170	GWh_{th}
	river and lake heat pump	-	-	19.076	MW_{el}
	wastewater heat pump	-	-	16.237	MW_{el}
	geothermal	22.367	-	-	GWh_{th}
	solar thermal	54.931	-	-	GWh_{th}
hydrogen	electrolysis	-	-	-	-

Table A7
Annual demand data (TWh) in 2050 used as input in Enertile

Country	DH demand (building on HT scenario in Ref. [46])	Demand other sectors [56] in TWh		
		Heat demand of decentralised heat pumps in buildings	Electricity demand	Hydrogen demand
Austria	18.5	19.3	89.9	27.0
Belgium	8.6	26.3	121.8	74.5
Bulgaria	6.4	6.3	37.7	7.8
Cyprus	0.0	0.3	5.0	0.2
Czechia	28.8	27.8	81.5	14.2
Germany	148.9	120.1	734.4	143.6
Denmark	21.2	11.2	53.2	0.3
Estonia	4.0	2.7	9.4	0.5
Spain	44.1	29.0	308.5	29.2
Finland	34.9	14.5	98.1	6.6
France	107.3	149.7	586.3	148.0
Greece	9.4	4.9	59.1	6.5
Croatia	3.4	3.6	17.0	0.8
Hungary	17.0	25.4	52.3	11.8
Ireland	1.3	11.2	32.8	2.4
Italy	89.3	74.7	372.3	50.4
Lithuania	6.9	3.6	13.9	5.5
Luxembourg	2.9	2.4	9.8	0.0
Latvia	4.9	3.0	10.0	0.0
Malta	0.0	0.0	2.5	0.1
Netherlands	24.7	40.9	172.7	56.7
Poland	59.3	40.5	223.5	23.4
Portugal	3.6	5.2	67.2	7.4
Romania	12.5	14.6	77.4	22.7
Sweden	65.8	25.1	169.9	11.4
Slovenia	1.7	19.3	18.0	0.0
Slovakia	6.9	26.3	39.4	9.2
Total	**732**	**708**	**3463**	**660**

Appendix B. – Additional results and sensitivity analysis

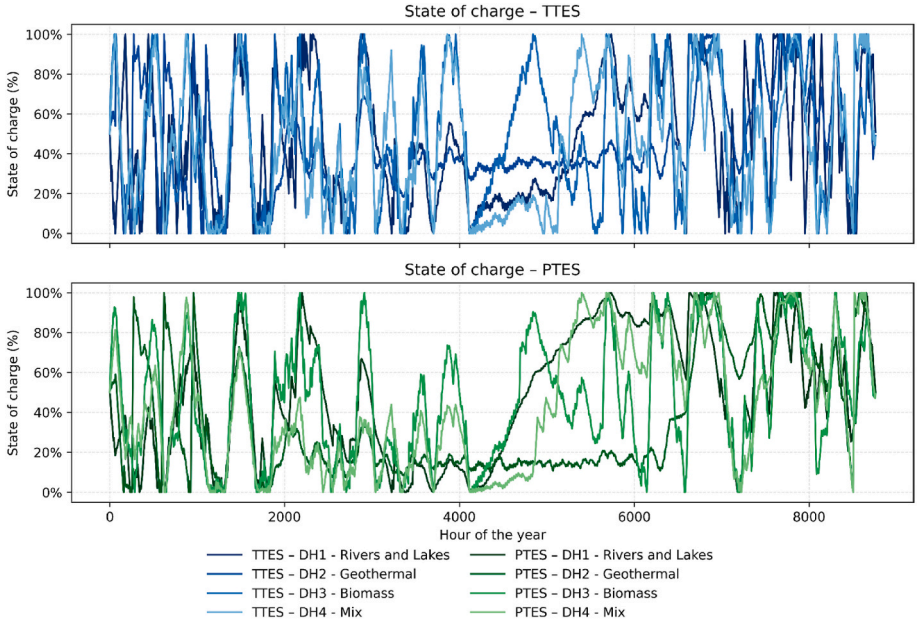

Fig. B1. Evolution of the state of charge of TES in different scenarios and DH types in Germany over the year.

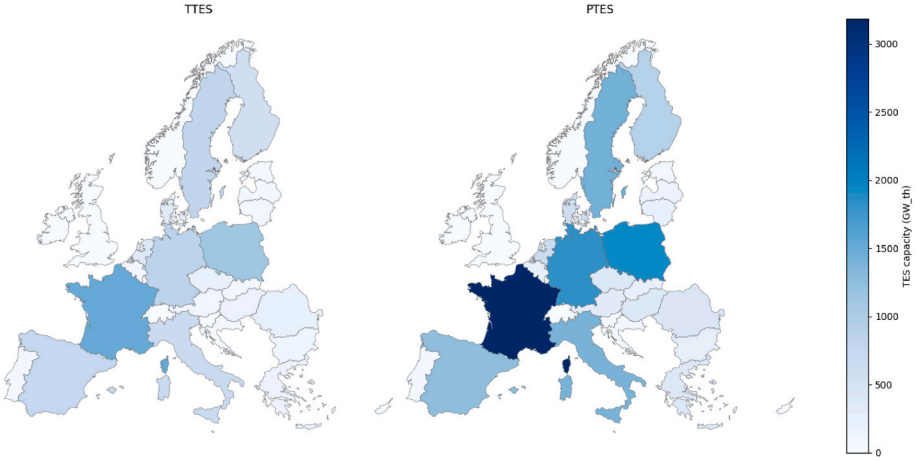

Fig. B2. Installed TES per model region, aggregated across the 4 DH type networks.

Table B1
Convergence and feasibility in the scenarios

	No-PTES	TTES	PTES	tolerance
Solver status	Optimal	Optimal	Optimal	-
Iterations	2409	929	1839	≤10,000
Relative Duality Gap[6]	$<10^{-9}$	3.3×10^{-9}	$<10^{-9}$	$\leq 10^{-6}$
Primal Residual	2.01×10^{-5}	5.63×10^{-5}	2.48×10^{-5}	$\leq 10^{-7}$
Dual Residual	1.89×10^{-2}	1.31×10^{-2}	4.10×10^{-2}	-
Complementarity	1.78×10^{-6}	4.04×10^{-6}	2.61×10^{-6}	$\leq 10^{-6}$
Solver time	69,771s	26,198	50,382s	<432,000 s

[6] Duality Gap = |Primal – Dual|/|Primal|.

Table B2
Assumptions and results of the sensitivity analysis

	Variation/Technology	Mix	S_CAPEX_PTES_low	S_CAPEX_PTES_high	S_bio_very_low	S_bio_low	S_bio_high	S_bio_very_high
Assumption	**Specific investment PTES (€/kWh)**	0.9	0.675	1.125	0.9	0.9	0.9	0.9
	Biomass price (€/MWh)	13	13	13	6.50	9.75	19.5	26
DH generation (TWh)	**Biomass CHP**	97.3	93.0	100.5	348.0	193.7	0.0	0.0
	Direct-electric	6.5	8.3	5.1	4.6	6.4	8.0	8.0
	Air heat pump	300.6	302.7	298.0	134.4	233.3	399.1	399.1
	Rivers and lakes heat pump	74.2	75.4	73.5	30.5	51.0	73.2	73.2
	Wastewater heat pump	57.4	56.0	59.1	45.2	52.9	56.5	56.5
	Hydrogen boiler	0.0	0.0	0.0	0.0	0.0	0.0	0.0
	Geothermal	77.1	77.1	77.1	77.1	77.1	77.1	77.1
	Industrial excess heat	16.2	16.2	16.2	16.2	16.2	16.2	16.2
	Solar thermal	73.2	73.2	73.2	73.2	73.2	73.2	73.2
	Waste CHP	46.1	46.1	46.1	46.1	46.1	46.1	46.1
	Curtailment	12.8	10.8	13.7	41.3	15.1	11.9	11.9
DH capacity (GW)	**Biomass CHP**	29.1	27.7	30.0	68.3	46.9	9.6	9.6
	Direct-electric	15.2	18.8	12.3	17.5	16.6	19.4	19.4
	Air heat pump	63.0	62.4	63.1	32.2	49.0	86.7	86.7
	Rivers and lakes heat pump	14.7	15.0	14.5	7.2	10.7	14.7	14.7
	Wastewater heat pump	14.7	13.8	15.3	12.3	13.6	14.7	14.7
	Hydrogen boiler	0.0	0.0	0.0	0.0	0.0	0.0	0.0
	Geothermal	8.8	8.8	8.8	8.8	8.8	8.8	8.8
	Industrial excess heat	1.8	1.8	1.8	1.8	1.8	1.8	1.8
	Solar thermal	48.2	48.2	48.2	48.2	48.2	48.2	48.2
	Waste CHP	0.0	0.0	0.0	0.0	0.0	0.0	0.0
	PTES (TWh)	16.8	23.1	13.8	9.2	12.6	23.9	23.9
	TTES (TWh)	0.0	0.0	0.0	0.0	0.0	0.0	0.0
Installed electric capacity (GW)	**Hydrogen**	148.8	149.8	148.2	144.8	143.9	156.7	156.7
	Electrolysis	296.9	297.3	296.6	271.9	285.4	307.4	307.4
	CSP	35.7	35.8	35.7	34.4	35.5	35.5	35.5
	PV roof	370.9	370.9	370.9	370.9	370.9	370.9	370.9
	PV utility scale	524.5	524.7	524.2	471.5	494.1	551.3	551.3
	Wind offshore	138.6	138.6	138.6	138.6	138.6	138.6	138.6
	Wind onshore	1078.2	1079.9	1077.5	964.9	1029.9	1115.4	1115.4
	Battery storage (TWh)	3.5	3.6	3.5	0.0	0.4	6.1	6.1

Appendix C. – Mathematical formulation of TES

Sets and Indices

- $t \in T = \{1, 2, \ldots, T\}$: The set of time steps (hours) in the modelled year, where T = 8760.

Parameters

- C^{cap}: The installed energy capacity of the storage.
- λ: The hourly loss factor, representing the fraction of stored energy lost per hour (proportional to the previous hour's SOC).

Variables

- SOC_t: SOC of the storage at the beginning of hour t.
- Q_t^{in}: energy charged into the storage during hour t.
- Q_t^{out}: energy discharged from the storage during hour t.
- X_t^{state}: Binary variable indicating the operational state of the storage during hour t (1 if charging, 0 if discharging/idle).

1. Mutually Exclusive Loading and Discharging

$$Q_t^{in} \leq C^{cap} * X_t^{state} \; \forall t \in T$$

$$Q_t^{out} \leq C^{cap} * \left(1 - X_t^{state}\right) \forall t \in T$$

2. Storage Capacity and Non-negativity Limits

The SOC cannot exceed the installed capacity and cannot be negative.

$$0 \leq SOC_t \leq C^{cap} \; \forall t \in T$$

With

$Q_t^{in} \geq 0;\ Q_t^{out} \geq 0$

3. Maximum Discharge per Hour

$0 \leq Q_t^{out} \leq C^{cap}\ \forall t \in T$

$0 \leq Q_t^{in} \leq C^{cap}\ \forall t \in T$

4. Energy Balance with Hourly Losses

The SOC for any given hour t+1 is the SOC of the previous hour, minus the losses (which are proportional to the previous hour's SOC), plus the net loaded energy.

$SOC_{t+1} = SOC_t * (1-\lambda) + Q_t^{in} - Q_t^{out}\ \forall t \in \{1, .., T-1\}$

5. First and Last Hour Boundary Conditions

For the first and last hours of the year, the SOC is fixed to exactly 50% of the installed capacity.

$SOC_1 = 0.5 * C^{cap}$

$SOC_T = 0.5 * C^{cap}$

Data availability

Model input data and key results supporting this study are available from the corresponding author upon reasonable request. The Enertile model code is proprietary to Fraunhofer ISI.

Data on DH type networks, including shape files and input data to the model are published at Fordatis - Research Data Repository of the Fraunhofer-Gesellschaft; https://doi.org/10.24406/fordatis/280.

References

[1] Staffell I, Pfenninger S. The increasing impact of weather on electricity supply and demand. Energy 2018;145:65–78. https://doi.org/10.1016/j.energy.2017.12.051.

[2] Heat Roadmap Europe. In: Heating and cooling: facts and figures," the transformation towards a; 2017 [Online]. Available: https://heatroadmap.eu/wp-content/uploads/2019/03/Brochure_Heating-and-Cooling_web.pdf.

[3] European Commission. An EU strategy on heating and cooling; 2016. Brussels. Availabe: eur-lex.europa.eu/legal-content/EN/TXT/PDF/?uri=CELEX:52016DC0051.

[4] The European Comission. In: The European Green deal; 2019. Brussels. [Online]. Available: https://eur-lex.europa.eu/legal-content/EN/TXT/?uri=celex%3A52019DC0640.

[5] Gabrielli P, Poluzzi A, Kramer GJ, Spiers C, Mazzotti M, Gazzani M. Seasonal energy storage for zero-emissions multi-energy systems via underground hydrogen storage. Renew Sustain Energy Rev 2020;12.

[6] IEA - International Energy Agency, "Managing the seasonal variability of electricity demand and supply,".

[7] Billerbeck A, et al. The race between hydrogen and heat pumps for space and water heating: a model-based scenario analysis. Energy Convers Manag 2024;299:117850. https://doi.org/10.1016/j.enconman.2023.117850.

[8] Lienhard N, Mutschler R, Leenders L, Rüdisüli M. Concurrent deficit and surplus situations in the future renewable Swiss and European electricity system. Energy Strategy Rev 2023;46:101036. https://doi.org/10.1016/j.esr.2022.101036.

[9] Lund PD, Lindgren J, Mikkola J, Salpakari J. Review of energy system flexibility measures to enable high levels of variable renewable electricity. Renew Sustain Energy Rev 2015;45:785–807. https://doi.org/10.1016/j.rser.2015.01.057.

[10] Gaafar N, Jürgens P, Sepúlveda Schweiger J, Kost C. System flexibility in the context of transition towards a net-zero sector-coupled renewable energy system—case study of Germany. Environ Res: Energy 2024;1(2):25007. https://doi.org/10.1088/2753-3751/ad5726.

[11] Brunner C, Deac G, Braun S, Zöphel C. The future need for flexibility and the impact of fluctuating renewable power generation. Renew Energy 2020;149:1314–24. https://doi.org/10.1016/j.renene.2019.10.128.

[12] Le TS, Nguyen TN, Bui D-K, Ngo TD. Optimal sizing of renewable energy storage: a techno-economic analysis of hydrogen, battery and hybrid systems considering degradation and seasonal storage. Appl Energy 2023;336:120817. https://doi.org/10.1016/j.apenergy.2023.120817.

[13] Tosatto A, Ochs F. Performance comparison of large-scale thermal energy storage and hydrogen as seasonal storage for achieving energy autarky in residential districts with different renovation levels. J Energy Storage 2024;98:113009. https://doi.org/10.1016/j.est.2024.113009.

[14] Yang Tianrun, Wen Liu, Kramer Gert Jan, Sun Qie. Seasonal thermal energy storage: a techno-economic literature review. Renew Sustain Energy Rev 2021;139.

[15] Xiang Y, Xie Z, Furbo S, Wang D, Gao M, Fan J. A comprehensive review on pit thermal energy storage: technical elements, numerical approaches and recent applications. J Energy Storage 2022;55:105716. https://doi.org/10.1016/j.est.2022.105716.

[16] Schmidt T, et al. Design aspects for large-scale pit and aquifer thermal energy storage for district heating and cooling. Energy Proc 2018;149:585–94. https://doi.org/10.1016/j.egypro.2018.08.223.

[17] Schüppler S, Fleuchaus P, Blum P. Techno-economic and environmental analysis of an Aquifer Thermal Energy Storage (ATES) in Germany. Geotherm Energy 2019;7(1). https://doi.org/10.1186/s40517-019-0127-6.

[18] Kök A, Billerbeck A, Manz P, Kranzl L. Achieving climate neutrality in district heating: the impact of system temperature levels on the supply mix of EU-27 in 2050. Energy 2025;315:134371. https://doi.org/10.1016/j.energy.2025.134371.

[19] Billerbeck A, et al. Integrating district heating potentials into European energy system modelling: an assessment of cost advantages of renewable and excess heat. Smart Energy 2024;15:100150. https://doi.org/10.1016/j.segy.2024.100150.

[20] Zeyen E, Hagenmeyer V, Brown T. Mitigating heat demand peaks in buildings in a highly renewable European energy system. Energy 2021;231:120784. https://doi.org/10.1016/j.energy.2021.120784.

[21] Mc Guire J, Petrović SN, Daly H, Rogan F, Smith A, Balyk O. Is District Heating a cost-effective solution to decarbonise Irish buildings? Energy 2024;296:131110. https://doi.org/10.1016/j.energy.2024.131110.

[22] Herpich P, Löffler K, Hainsch K, Hanto J, Moskalenko N. 100% renewable heat supply in Berlin by 2050 – a model-based approach. Appl Energy 2024;375:124122. https://doi.org/10.1016/j.apenergy.2024.124122.

[23] Sihvonen V, et al. Role of power-to-heat and thermal energy storage in decarbonization of district heating. Energy 2024;305:132372. https://doi.org/10.1016/j.energy.2024.132372.

[24] Zhou D, Li K, Gao H, Tatomir A, Sauter M, Ganzer L. Techno-economic assessment of high-temperature aquifer thermal energy storage system, insights from a study case in Burgwedel, Germany. Appl Energy 2024;372:123783. https://doi.org/10.1016/j.apenergy.2024.123783.

[25] Vilén K, Ahlgren EO. Seasonal large-scale thermal energy storage in an evolving district heating system – Long-term modeling of interconnected supply and demand. Smart Energy 2024;15:100156. https://doi.org/10.1016/j.segy.2024.100156.

[26] Bloess A, Schill W-P, Zerrahn A. Power-to-heat for renewable energy integration: a review of technologies, modeling approaches, and flexibility potentials. Appl Energy 2018;212:1611–26. https://doi.org/10.1016/j.apenergy.2017.12.073.

[27] Bernath C, Deac G, Sensfuß F. Impact of sector coupling on the market value of renewable energies – a model-based scenario analysis. Appl Energy 2021;281:115985.
[28] Brown T, Schlachtberger D, Kies A, Schramm S, Greiner M. Synergies of sector coupling and transmission reinforcement in a cost-optimised, highly renewable European energy system. Energy 2018;160:720–39. https://doi.org/10.1016/j.energy.2018.06.222.
[29] Ryan E, McDaniel B, Kosanovic D. Application of thermal energy storage with electrified heating and cooling in a cold climate. Appl Energy 2022;328:120147. https://doi.org/10.1016/j.apenergy.2022.120147.
[30] Burkhardt A, Billerbeck A, Bernath C, Manz P, Deac G, Held A. The role of thermal energy storage in market integration of variable renewable electricity - a German case Study. *2024*. https://doi.org/10.1109/EEM60825.2024.10608961.
[31] Lux B, et al. The role of hydrogen in a greenhouse gas-neutral energy supply system in Germany. Energy Convers Manag 2022;270:116188. https://doi.org/10.1016/j.enconman.2022.116188.
[32] Lux B, Gegenheimer J, Franke K, Sensfuß F, Pfluger B. Supply curves of electricity-based gaseous fuels in the MENA region. Comput Ind Eng 2021;162:107647. https://doi.org/10.1016/j.cie.2021.107647.
[33] Sifnaios I, Sneum DM, Jensen AR, Fan J, Bramstoft R. The impact of large-scale thermal energy storage in the energy system. Appl Energy 2023;349:121663. https://doi.org/10.1016/j.apenergy.2023.121663.
[34] Ceruti A, Lambert J, Spliethoff H. Integrating renewable energy and thermal storage in district heating networks: a design optimization approach. Energy Convers Manag 2025;345:120323. https://doi.org/10.1016/j.enconman.2025.120323.
[35] Heinen S, Turner W, Cradden L, McDermott F, O'Malley M. Electrification of residential space heating considering coincidental weather events and building thermal inertia: a system-wide planning analysis. Energy 2017;127:136–54. https://doi.org/10.1016/j.energy.2017.03.102.
[36] Lu H, Zhang H, Lu S. Revisiting the role of thermal energy storage in low-temperature electrified district heating systems. IET Energy Syst Integration 2024;6(S1):845–61. https://doi.org/10.1049/esi2.12174.
[37] Narula K, de Oliveira Filho F, Villasmil W, Patel MK. Simulation method for assessing hourly energy flows in district heating system with seasonal thermal energy storage. Renew Energy 2020;151:1250–68. https://doi.org/10.1016/j.renene.2019.11.121.
[38] Gao M, Furbo S, Kong W, Wang D, Fan J. Validation and optimization of a solar district heating system with large scale heat storage. J Clean Prod 2024;484:144360. https://doi.org/10.1016/j.jclepro.2024.144360.
[39] Burkhardt A, Frömel M, Deac G, Billerbeck A. Modeling thermal energy storage — the effect of self-discharge rates on dispatch. 2025. https://doi.org/10.1109/EEM64765.2025.11050343.
[40] Mantegna G, Ricks W, Manocha A, Patankar N, Mallapragada D, Jenkins J. Establishing best practices for modeling multi-day energy storage in deeply decarbonized energy systems. Environ Res: Energy 2024;1(4):45014. https://doi.org/10.1088/2753-3751/ad96bd.
[41] Schauß C., Schledorn A., Kähler T., Brown T. Assessing the impact of pit thermal energy storage on flexibility in sector-coupled energy systems. 2025 21st international conference on the European Energy Market (EEM), Lisbon, Portugal; 2025. p. 1–8. Assessing the Impact of Pit Thermal Energy Storage on Flexibility in Sector-Coupled Energy Systems.pdf.
[42] Bernath C, Deac G, Sensfuß F. Influence of heat pumps on renewable electricity integration: germany in a European context. Energy Strategy Rev 2019;26:100389. https://doi.org/10.1016/j.esr.2019.100389.
[43] Lux B, Schneck N, Pfluger B, Männer W, Sensfuß F. Potentials of direct air capture and storage in a greenhouse gas-neutral European energy system. Energy Strategy Rev 2023;45:101012. https://doi.org/10.1016/j.esr.2022.101012.
[44] Pan X, et al. Long-term thermal performance analysis of a large-scale water pit thermal energy storage. J Energy Storage 2022;52:105001. https://doi.org/10.1016/j.est.2022.105001.
[45] IEA-ECES. Applications of thermal energy storage in the energy transition: benchmarks and developments; 2018. Available: Applications-of-Thermal-Energy-Storage-in-the-Energy-Trenasition-Annex-30_Public-Report.pdf.
[46] Manz P, et al. Spatial analysis of renewable and excess heat potentials for climate-neutral district heating in Europe. Renew Energy 2024;224:120111. https://doi.org/10.1016/j.renene.2024.120111.
[47] Sifnaios I, Gauthier G, Trier D, Fan J, Jensen AR. Dronninglund water pit thermal energy storage dataset. Sol Energy 2023;251:68–76. https://doi.org/10.1016/j.solener.2022.12.046.
[48] Sporleder M, Rath M, Xu Y, van Beek M, Ragwitz M. Utilizing historical operating data to increase accuracy for optimal seasonal storage integration and planning. In: Proceedings of ECOS. 2023. ECOS: Template for Manuscripts; 2023. p. 2023.
[49] Sporleder M, Rath M, Ragwitz M. Solar thermal vs. PV with a heat pump: a comparison of different charging technologies for seasonal storage systems in district heating networks. Energy Convers Manag X 2024;22:100564. https://doi.org/10.1016/j.ecmx.2024.100564.
[50] Moradi-Shahrbabak Z, Jadidoleslam M. A new index for techno-economical comparison of storage technologies considering effect of self-discharge. IET Renewable Power Gen 2023;17(7):1699–712. https://doi.org/10.1049/rpg2.12704.
[51] Gea-Bermúdez Juan, et al. The role of sector coupling in the green transition: a least-cost energy system development in northern-central Europe towards 2050. Appl Energy 2021;289:116685. https://doi.org/10.1016/j.apenergy.2021.116685 [Online]. Available:.
[52] Guerra OJ, Zhang J, Eichman J, Denholm P, Kurtz J, Hodge B-M. The value of seasonal energy storage technologies for the integration of wind and solar power. Energy Environ Sci 2020;13(7):1909–22. https://doi.org/10.1039/D0EE00771D.
[53] McKenna R, Fehrenbach D, Merkel E. The role of seasonal thermal energy storage in increasing renewable heating shares: a techno-economic analysis for a typical residential district. Energy Build 2019;187:38–49. https://doi.org/10.1016/j.enbuild.2019.01.044.
[54] Henning H-M, Palzer A. A comprehensive model for the German electricity and heat sector in a future energy system with a dominant contribution from renewable energy technologies—Part I: methodology. Renew Sustain Energy Rev 2014;30:1003–18. https://doi.org/10.1016/j.rser.2013.09.012.
[55] Danish Energy Agency. In: New chapter on long term energy storage in the Technology Catalogue: Technology brief; 2025 [Online]. Available: https://ens.dk/media/6445/download.
[56] Dröscher T, et al. Potentials and levels for the electrification of space heating in buildings: final report. Brussels: Directorate-General for Energy; 2023. https://doi.org/10.2833/282341 [Online]. Available:.
[57] Bacquet A, et al. Overview of district heating and cooling markets and regulatory frameworks under the revised renewable energy directive: main report : final version. Brussels: Tilia GmbH et al.; 2021 [Online]. Available: https://op.europa.eu/o/opportal-service/download-handler?identifier=4e28b0c8-eac1-11ec-a534-01aa75ed71a1&format=pdf&language=en&productionSystem=cellar&part=.
[58] Mandel T, Kranzl L, Popovski E, Sensfuß F, Müller A, Eichhammer W. Investigating pathways to a net-zero emissions building sector in the European Union: what role for the energy efficiency first principle? Energy Effic 2023;16(4). https://doi.org/10.1007/s12053-023-10100-0.
[59] Kranzl L, et al. "Renewable space heating under the revised renewable energy directive: ENER/C1/2018-494. Brussels. [Online]. Available: https://data.europa.eu/doi/10.2833/525486; 2021.
[60] Hummel M, Müller A, Forthuber S, Kranzl L, Mayr B, Haas R. How cost-efficient is energy efficiency in buildings? A comparison of building shell efficiency and heating system change in the European building stock. Energy Effic 2023;16(5). https://doi.org/10.1007/s12053-023-10097-6.
[61] Tsiropoulos I, Nijs W, Tarvydas D, Ruiz P. Towards net-zero emissions in the EU energy system by 2050: insights from scenarios in line with the 2030 and 2050 ambitions of the European Green Deal. Luxembourg: JRC technical reports JRC118592; 2020. Europäische Kommission.
[62] Schlemminger M, et al. Flexibility is the key to decarbonizing heat supply: a case study based on the German energy system. Energy Convers Manag 2025;324:119300. https://doi.org/10.1016/j.enconman.2024.119300.
[63] Jåstad EO, Bolkesjø TF, Trømborg E, Rørstad PK. The role of woody biomass for reduction of fossil GHG emissions in the future North European energy sector. Appl Energy 2020;274:115360. https://doi.org/10.1016/j.apenergy.2020.115360.
[64] Danish Energy Agency. In: Technology data generation of electricity and district heating: version 12; 2022 [Online]. Available: https://ens.dk/media/3274/download.
[65] L. L. Gurobi optimization, Parameter Reference. [Online]. Available: https://docs.gurobi.com/projects/optimizer/en/current/reference/parameters.html (accessed: March. 23 2026).
[66] Lux B, Frömel M, Resch G, Hasengst F, Sensfuß F. Effects of different renewable electricity diffusion paths and restricted european cooperation on Europe's hydrogen supply. Energy Strategy Rev 2024;56:101589. https://doi.org/10.1016/j.esr.2024.101589.